COMPUTATIONAL MODEL FOR SUPERCONDUCTING TOROIDAL-FIELD MAGNETS FOR A TOKAMAK REACTOR*

L.R. Turner and M.A. Abdou

Argonne National Laboratory
Argonne, IL 60439

Paper presented at and published in the Proceedings of the 7th Symposium on Engineering Problems of Fusion Research, 25-28 October 1977, Knoxville, TN

*Work supported by the U.S. Department of Energy

COMPUTATIONAL MODEL FOR SUPERCONDUCTING TOROIDAL-FIELD MAGNETS FOR A TOKAMAK REACTOR*

L. R. Turner and M. A. Abdou
Argonne National Laboratory
Argonne, Illinois 60439

A23

Summary

A computational model for predicting the performance characteristics and cost of superconducting toroidal-field (TF) magnets in tokamak reactors is presented. The model can be used to compare the technical and economic merits of different approaches to the design of TF magnets for a reactor system. The model has been integrated into the ANL Systems Analysis Program. Samples of results obtainable with the model are presented.

Introduction

An integrated systems computer program for simulation of tokamak power plants has been developed at ANL.[1] The program consists of modular units with each unit corresponding to a reactor subsystem. This report describes a model that has been developed for the toroidal-field (TF) coils. The model is described in more detail in reference 2.

The Model in Outline

The TF coils are taken to be of the constant tension shape;[3] the shape is calculated by the approximate method of Moses and Young.[4]

Several material choices are permitted in specifying the magnet. The magnet may be superconducting or conventional; if it is superconducting, the superconductor may be NbTi or a hybrid with NbTi in the low-field turns and Nb_3Sn in the high-field turns. The superconductor may be graded or ungraded. The magnet may be cryostable or intrinsically stable; the stabilizer may be graded or ungraded.

The simplified flow diagram in Figure 1 shows how the model operates. The maximum magnetic field and the space requirements inside the TF coil are first specified; from these the coil thickness is estimated and the inner and outer mid-radii R_1 and R_2 of the coil calculated. At this point the choice between cryostable or intrinsically stable coils occurs. In either case, the choice between NbTi or hybrid coils is made at this point on the basis of the maximum field. The critical current density, J_c, and the cross-sectional area, A_{sc}, complete the specification of the superconductor.

For an intrinsically stable conductor, the ratio of copper to superconductor is specified; for a cryostable conductor the amount of copper is determined from cryostability considerations involving heat transfer to the helium and electrical resistivity. Since the magnetoresistivity and radiation-induced resistivity vary across the thickness of a coil, the copper can be graded. The amount of stainless steel support material is determined by the specified allowable stress or strain and the tension in the coil.

From the total cross section the corresponding thickness is calculated. If it differs too much from the previous estimate of thickness, the calculation must be iterated until it converges. After it does, the circumference is calculated; and from it the total amount of superconductor, copper and stainless steel in the system. Finally, stored energy and costs are calculated.

* Work supported by the U.S. Department of Energy.

The Model in Detail

Parameters Specified

Certain parameters must be specified initially: the peak magnetic field, B_{max}, the design temperature, T, the outer radius of the inner TF coil leg and the inner radius of the outer TF coil leg. These latter two are determined by the space needs for the blanket and shield. The design temperature T is the sum of the operating temperature, generally 4.2 K, and the temperature safety margin, generally 0.5 K.

Another parameter to be specified is the permissible stress or strain in the conductor. For a Nb_3Sn-Cu composite conductor, the strain is limited by the brittleness of the Nb_3Sn; but for a NbTi-Cu composite conductor, it is limited only by the strain-induced resistivity of the copper.

The Superconductor

Two kinds of coils are envisioned; for fields B_{max} up to 8 or 10 T, NbTi is used. For higher values of B_{max}, hybrid coils are considered, with NbTi in the outer turns and Nb_3Sn in the inner turns where the field is higher. The choice is an input option. In either case, the total current NnI is given by Ampere's Law.

Although superconducting TF coils for a tokamak reactor would almost certainly be cryostable, it may prove interesting to compare cryostable and intrinsically stable coils; so provision is made in the magnet model for intrinsically stable coils as well.

Critical Current Density. For NbTi, the critical current density as a function of temperature T in Kelvin and field B in Tesla is shown in Figure 2. The data in Figure 2 are fit by the expression

$$J_c = (T_c - T)\,(3.352 - 0.3607\,B + 11.929/T) \times 10^4 \text{ A/cm}^2 \quad (1)$$

where the critical temperature T_c can be found by

$$T_c = 8.56\,(1 - B/14.7)^{1/2} \quad (2)$$

Over the region 1 T ≤ B ≤ 11 T, 3 K ≤ T ≤ 6 K, $T_c - T \geq 1$ K, Eq. (1) fits the data to 10% or better.

There is considerable uncertainty as to what values of J_c can be obtained in practical Nb_3Sn conductors. We use the expression

$$J_c = (35.55 - 4.25\,B + 0.1375\,B^2)\,(0.739 + 0.144\,T - 0.0196\,T^2) \times 4.74 \times 10^4 \text{ A/cm}^2 \quad (3)$$

Cross-Sectional Area. For a cryostable NbTi magnet, the cross-sectional area of superconductor is given by

$$A_{NbTi} = NnI/J_c \quad (4)$$

where J_c is found from Eq. (1) with $B = B_{max}$.

Few intrinsically stable magnets operate at the short-sample value of J_c. Consequently, the area found

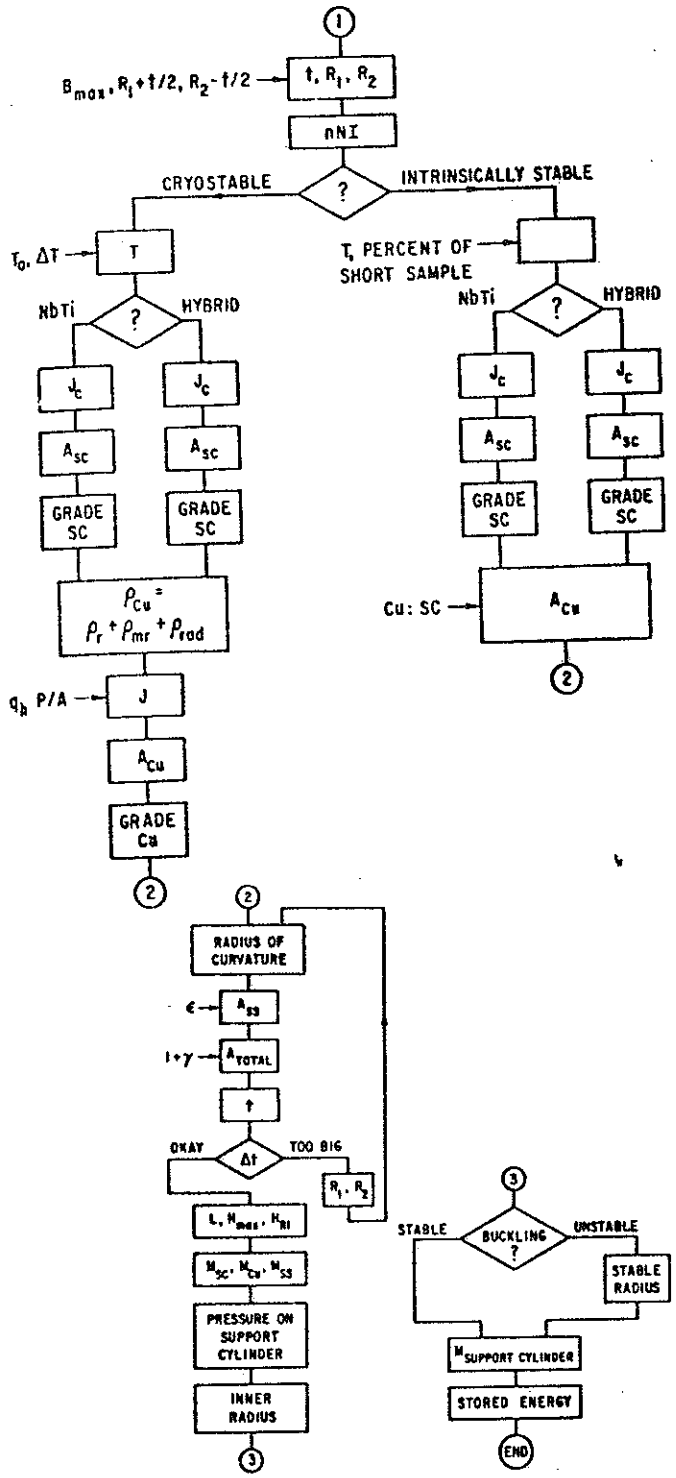

Figure 1. Simplified Flow Diagram for the TF Magnet Model.

by Eq. (4) should be increased for an intrinsically stable magnet.

For hybrid coils, the fraction of current to be carried by the NbTi is taken to be B_{Cut}/B_{max}, where B_{Cut} is the highest field at which NbTi is to be used in the hybrid magnet. B_{Cut} has been taken to be 8 T in the model. The cross-sectional areas are given by Eq. (4), but evaluated for the fraction of the current in each.

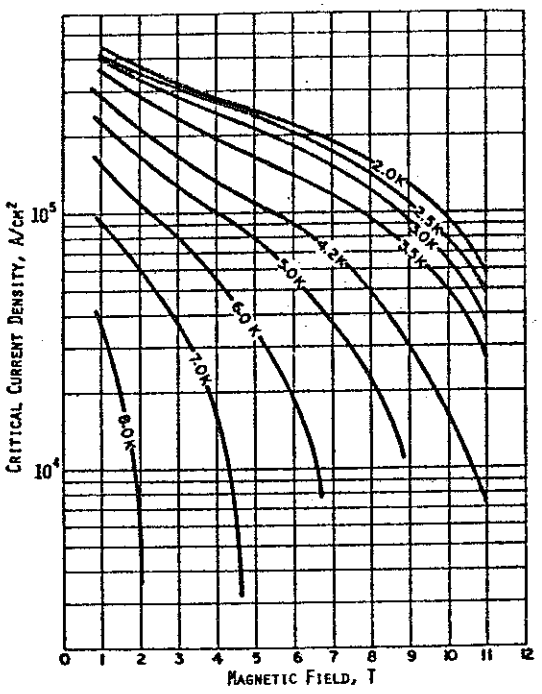

Figure 2. J-H Curve for NbTi Versus Temperature

Grading the Superconductor. The cross-sectional areas determined from Eq. (4) assume that the current density in the superconductors throughout the coils is that which can be attained at the highest fields. Grading the superconductor by including less where the field is lower can save cost, weight and space without impairing the performance of the magnet.

The Copper Stabilizer

A cryostable magnet must obey the cryostability condition

$$J^2 \rho A_{Cu} = q_h p \tag{5}$$

where J is the current density in the copper of a composite conductor which has gone normal, ρ is the total resistivity of the copper, A_{Cu} is the cross-sectional area of the copper, p is its wetted perimeter and q_h is the effective heat flux into the helium. To determine J and thus

$$A_{cu} = NnI/J \tag{6}$$

we consider each of these factors in turn.

The total resistivity is the sum of the intrinsic resistivity, ρ_o, the magnetoresistivity, ρ_{mr}, and the radiation induced resistivity, ρ_{rad}. There is uncertainty in the value $\rho_o = 6 \times 10^{-9}$ Ω cm, but it is dominated by ρ_{mr} and ρ_{rad} anyway. The magnetoresistivity is given by

$$\rho_{mr} = 4.55 \times 10^{-9} \text{ Ω cm} \cdot B \tag{7}$$

and the radiation-induced resistivity[5] by

$$\rho_{rad} = 3 \times 10^{-7} \ (1 - \exp(-563d)) \text{ Ω cm} \tag{8}$$

where d is the total atomic displacements.

For a sheet conductor of the kind described in the ANL/EPR design,[6] the ratio A_{Cu}/p equals the thickness for a 50% wetted surface.

In Eq. (5), q_h includes the effect of heat transfer along the conductor or between turns as well as into the helium. So interpreted q_h may be less than 0.06 W/cm^2 or greater than 2.2 W/cm^2, but it is customary to take $q_h = 0.35$ W/cm^2.

With these factors specified, J can be found from Eq. (5) and A_{Cu} from Eq. (6).

Grading the Copper. The resisitivty of the copper is dominated by the magnetoresistivity and the radiation-induced resistivity, both of which are smaller for the outer turns than for the inner ones. Thus, there can be savings in grading the copper as there are in grading the superconductor.

Stainless Steel Reinforcement for Coils

Enough stainless steel reinforcement must be included with the coils to withstand the tension, τ, in the coils and limit the stress or strain in the coils to the allowable value.

The tension is related to the stresses through the relation

$$\tau = A_{Cu}\,\sigma_{Cu} + A_{SS}\,\sigma_{SS} \qquad (9)$$

where σ_{Cu} and σ_{SS} are the allowable stresses in the copper and stainless steel respectively. In general, a specified σ_{Cu} and σ_{SS} occur simultaneously only if the coil is wound with the copper in precompression and the stainless steel in pretension. The model calculates the required prestresses before and after cooldown and confirms that they do not exceed σ_{Cu} or σ_{SS}.

Alternatively, the allowable strain, ε, can be specified rather than the stresses σ_{Cu} and σ_{SS}; in this case no pretension is assumed.

Geometry of Coils

Moses and Young[4] have shown how the geometrical parameters of a constant-tension coil shown in Figure 3 can be generated numerically. We have integrated their expression for a family of parametric values, and fit the results as functions of R_1 and R_2.

Iteration for Thickness, t

The total area of the coils exceeds that occupied by the superconductor, copper and stainless steel by a factor of $1 + \gamma$, corresponding to helium space, cryostat walls, insulation, etc. Assuming no gaps between coils in the inner leg, we find the thickness, t, by

$$t = (1 + \gamma)\,(A_{SC} + A_{Cu} + A_{SS})/2\pi R_1 \qquad (10)$$

The model requires iteration over the coil thickness t. It is necessary to take some initial value for t and iterate through the calculation until the value for t converges. Then R_1 and R_2 can be found, and from them the other shape parameters of Figure 3.

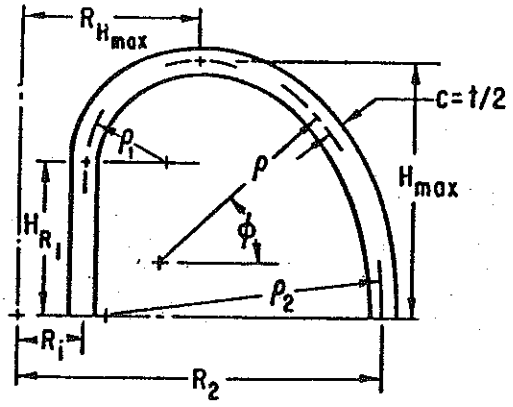

Figure 3. Geometric Parameters for a Constant-Tension Coil

Magnet Anneal

Most of the radiation damage in the superconductor and normal metal can be recovered by warming up the magnet to near room temperature. There is a strong incentive to reduce the shield thickness, permit a higher radiation level at the magnet, and anneal the magnet periodically. However, magnet warmup and cooldown require two to three months of plant downtime. Thus, there is an optimum time span between magnet anneals. At present the program permits specifying t_a in one of two modes: either t_a is an input variable, or t_a is defined to be equal to the lifetime of the first wall.

The Support Cylinder

There is a compressive force pushing all TF coils toward the axis of the tokamak; this force must be taken up by the support cylinder, a hollow cylinder of stainless steel. The cylinder must be thick enough that the stresses resulting from that force do not exceed the peak acceptable circumferential stress σ_{max}, (typically 3.45 x 10^{11} Nt/m^2 or 50,000 psi). The support cylinder must also be thick enough to be stable against buckling.

Stored Energy

The stored energy of the TF coil system is an important parameter in its own right; in addition, attempts have sometimes been made to scale the costs of magnet systems according to stored energy.

The energy is found from the volume integral

$$E = \frac{1}{2\mu_o}\int B^2\,dV.$$

We assume that B is zero outside the coils and has a 1/r dependence inside. We approximate h (r), the half height as a function of radius, by a parabola passing through the points (R_1, H_{R_1}) and $(R_2, 0)$ and of height H_{max}.

$$E = \frac{2\,B_{max}^2\,(R_1 + t/2)^2}{\mu_o\,(R_2 - R_1)^2}\,[R_2\,(H_{R_1}\,R_2 - 2R_1\,\Omega) \qquad (11)$$

$$\ln\,(R_2/R_1) + (R_2^2 - R_1^2)\,\Omega - (R_2 - R_1)\,H_{R_1}/2]$$

with $\Omega = H_{max}\,(1 + \sqrt{1 - H_{R_1}/H_{max}})$.

TF Magnet Costs

The volume of superconductor, copper stabilizer or stainless steel reinforcement is found by multiplying the circumference by the cross-sectional area, incorporating grading if appropriate. Multiplication by the density then yields the mass. The cost of materials is calculated assuming unit material costs. The electrical insulation, superinsulation and dewar are costed on the basis of volume or area. The magnet cost is

equal to the material plus fabrication and winding cost, and at present, is taken as four times the material cost.

The refrigeration load is calculated as the sum of the nuclear energy deposition and thermal leakage. The refrigeration load is converted to electric power requirements using a multiplicative factor of 300 for 4.2 K cooling and 500 for 3 K cooling. The electric power requirements are passed into another part of the system code that calculates the plant net electric power output.

Results

The model was used to study how magnet parameters vary with major radius, peak magnetic field and material properties. One or two parameters were changed for each study. During variation with major radius, the aspect ratio R/a was held at a constant value of three.

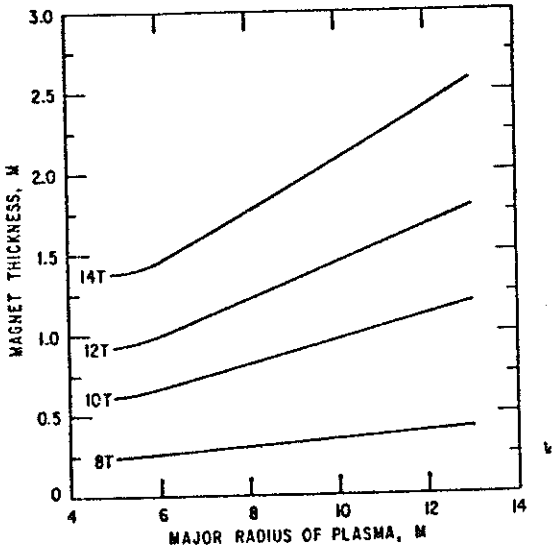

Figure 4. Magnet Thickness as a Function of Major Radius at Several Values for the Maximum Magnetic Field.

Coil Thickness

The coil thickness is shown in Figure 4 as a function of major radius for several peak fields. The tension increases with both radius and field, and consequently the coils must be thicker to withstand the tension. Moreover, the lower permissible strain with hybrid coils accentuates the increase in thickness with field.

Variation of coil thickness with allowable strain is shown in Figure 5 for an 8 T field and in Figure 6 for a 12 T field. In each case, major radii of 5 m to 13 m are treated. The rapid increase in thickness as the strain is decreased below 0.1% is striking. For a 12 T field, 0.05% strain, and an aspect ratio of 3, there is not enough room for TF coils with major radius of 5 m or less. Under the same conditions there is not enough room for the support cylinder in reactors with 7 m or less major radius.

Stored Energy and Cost

The energy stored in the TF coil system is shown in Figure 7 (and the cost in Figure 8) as functions of major radius for fields between 8 T and 14 T. Here too the rapid increase with both field and major radius is evident.

The cost as a function of allowable strain for major radii between 5 m and 13 m is shown in Figure 9 for a field of 8 T and in Figure 10 for a field of 12 T. The increased thickness required for low strain, shown in Figure 5 and Figure 6, represent increased material requirements and thus increased cost.

References

1. M. A. Abdou, et al., "Parametric Systems Analyses for Tokamak Power Plants," Argonne National Laboratory, ANL/FPP/TM-97 (October, 1977).

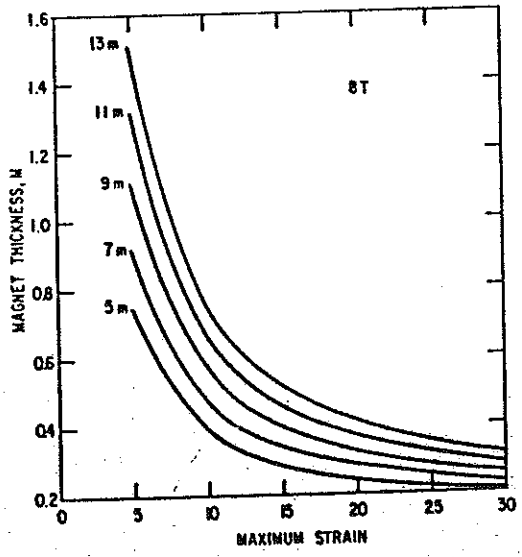

Figure 5. Sensitivity of the Magnet Thickness to the Permissible Strain. Results are shown for a Maximum Magnetic Field of 8 T and Several Values for the Major Radius.

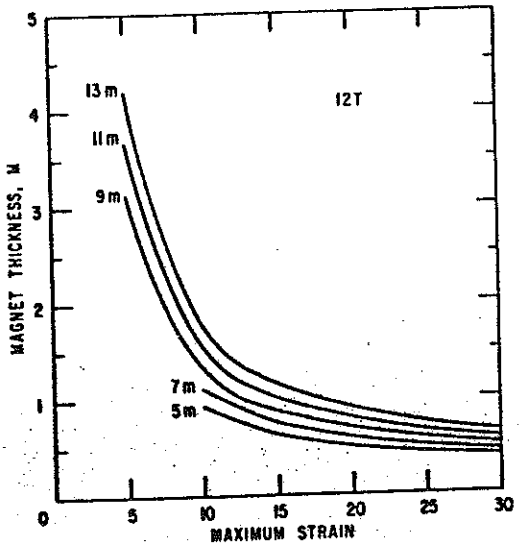

Figure 6. Sensitivity of the Magnet Thickness to the Permissible Strain. Results are Shown for a Maximum Magnetic Field of 12 T and Several Values for the Major Radius.

2. L. R. Turner and M. A. Abdou, "Conceptual Model for Superconducting Toroidal Field Magnet for a Tokamak Reactor," Argonne National Laboratory, ANL/FPP/TM-88 (August, 1977).

3. W. M. Stacey, Jr., et al., "Tokamak Experimental Power Reactor Studies," Argonne National Laboratory, ANL/CTR-75-2 (June, 1975).

4. R. W. Moses, Jr. and W. C. Young, "Analytic Expressions for Magnetic Forces on Sectored Toroidal Coils," Proc. of 6th Symposium on Engineering Problems of Fusion Research (1975) pp. 917-921.

5. M. A. Abdou, "Radiation Considerations for Superconducting Fusion Magnets," International Meeting on Radiation Effects on Superconductivity, Argonne Illinois (1977); to be published in *J. Nucl. Materials*.

6. L. R. Turner, et al., "Superconducting Magnet Systems for the ANL/EPR Design," Proc. of Seventh Symposium on Engineering Problems of Fusion Research (October, 1977).

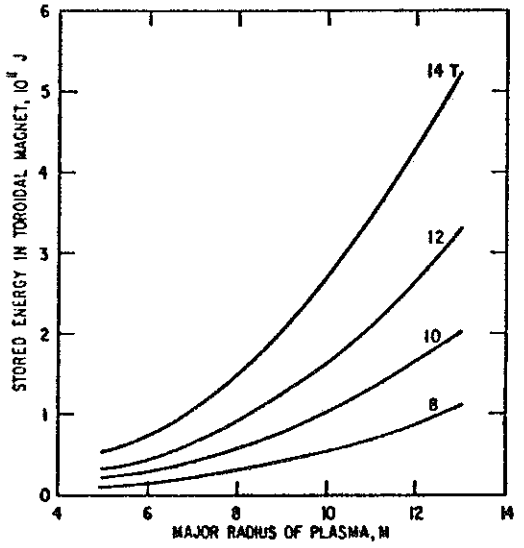

Figure 7. Stored Energy as a Function of the Major Radius at Several Values of the Maximum Magnetic Field.

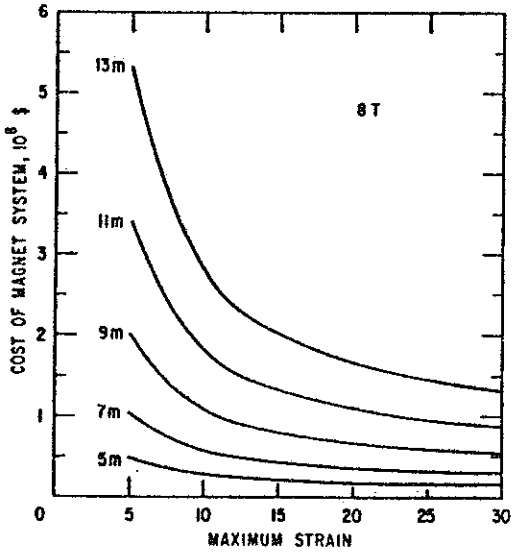

Figure 9. Sensitivity of the Magnet Cost to the Permissible Strain for a Maximum TF Field of 8 T.

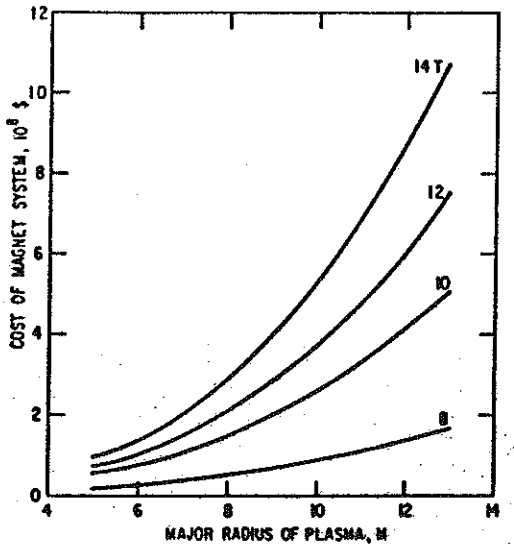

Figure 8. Cost of the TF Magnet as a Function of Reactor Size and Maximum Field.

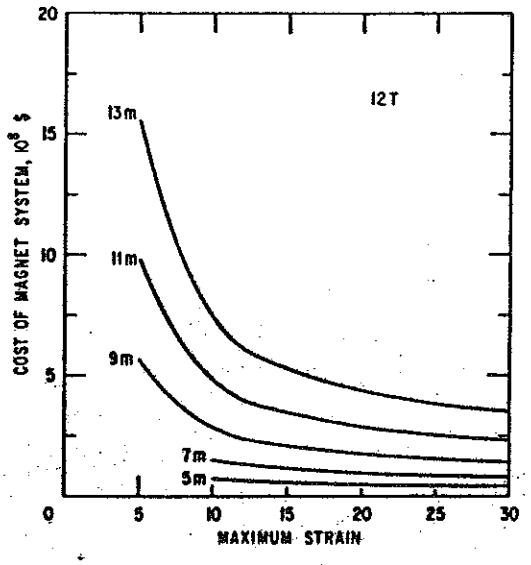

Figure 10. Sensitivity of the Magnet Cost to the Permissible Strain for a Maximum TF Field of 12 T.